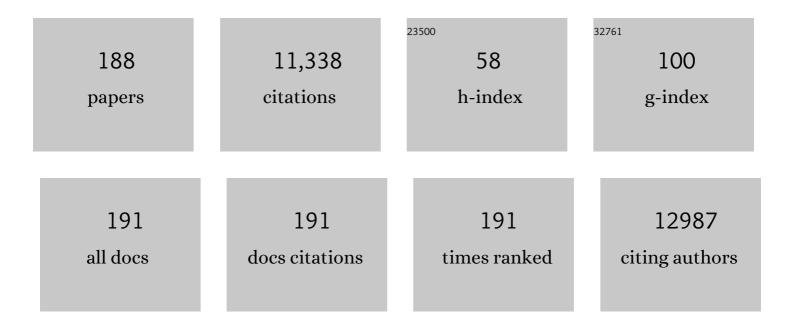
## List of Publications by Year in descending order

Source: https://exaly.com/author-pdf/5139639/publications.pdf Version: 2024-02-01



#	Article	IF	CITATIONS
1	Redox Defect Thermochemistry of FeAl <sub>2</sub> O <sub>4</sub> Hercynite in Water Splitting from First-Principles Methods. Chemistry of Materials, 2022, 34, 519-528.	3.2	11
2	Predicting Oxygen Off-Stoichiometry and Hydrogen Incorporation in Complex Perovskite Oxides. Chemistry of Materials, 2022, 34, 510-518.	3.2	7
3	A Computational Framework to Accelerate the Discovery of Perovskites for Solar Thermochemical Hydrogen Production: Identification of Gd Perovskite Oxide Redox Mediators. Advanced Functional Materials, 2022, 32, .	7.8	7
4	Predictive energetic tuning of C-Nucleophiles for the electrochemical capture of carbon dioxide. IScience, 2022, 25, 103997.	1.9	4
5	Ab initio screening of refractory nitrides and carbides for high temperature hydrogen permeation barriers. Journal of Nuclear Materials, 2022, 563, 153611.	1.3	3
6	Bond-Valence Parameterization for the Accurate Description of DFT Energetics. Journal of Chemical Theory and Computation, 2022, 18, 3257-3267.	2.3	3
7	How the Bioinspired Fe <sub>2</sub> Mo <sub>6</sub> S <sub>8</sub> Chevrel Breaks Electrocatalytic Nitrogen Reduction Scaling Relations. Journal of the American Chemical Society, 2022, 144, 12800-12806.	6.6	29
8	Determining Michael acceptor reactivity from kinetic, mechanistic, and computational analysis for the base-catalyzed thiol-Michael reaction. Polymer Chemistry, 2021, 12, 3619-3628.	1.9	9
9	Reduction of N <sub>2</sub> to Ammonia by Phosphate Molten Salt and Li Electrode: Proof of Concept Using Quantum Mechanics. Journal of Physical Chemistry Letters, 2021, 12, 1696-1701.	2.1	6
10	Kinetics of Hydride Transfer from Catalytic Metal-Free Hydride Donors to CO <sub>2</sub> . Journal of Physical Chemistry Letters, 2021, 12, 2306-2311.	2.1	19
11	Mechanistic Studies of Styrene Production from Benzene and Ethylene Using [(η <sup>2</sup> -C <sub>2</sub> H <sub>4</sub> ) <sub>2</sub> Rh(μ-OAc)] <sub>2</sub> as Catalyst Precursor: Identification of a Bis-Rh <sup>I</sup> Mono-Cu <sup>II</sup> Complex As the Catalyst. ACS Catalysis, 2021, 11, 5688-5702.	5.5	9
12	Machine Learning Guided Synthesis of Multinary Chevrel Phase Chalcogenides. Journal of the American Chemical Society, 2021, 143, 9113-9122.	6.6	22
13	Visible-Light Photoinitiation of (Meth)acrylate Polymerization with Autonomous Post-conversion. Macromolecules, 2021, 54, 7702-7715.	2.2	2
14	Atomic layer deposited boron nitride nanoscale films act as high temperature hydrogen barriers. Applied Surface Science, 2021, 565, 150428.	3.1	9
15	Diazaphospholenes as reducing agents: a thermodynamic and electrochemical DFT study. Physical Chemistry Chemical Physics, 2021, 23, 17794-17802.	1.3	7
16	Electrocatalytic Reduction of CO <sub>2</sub> to CO over Ag(110) and Cu(211) Modeled by Grand-Canonical Density Functional Theory. Journal of Physical Chemistry C, 2021, 125, 23773-23783.	1.5	26
17	Computationally Accelerated Discovery and Experimental Demonstration of Gd0.5La0.5Co0.5Fe0.5O3 for Solar Thermochemical Hydrogen Production. Frontiers in Energy Research, 2021, 9, .	1.2	12
18	Altering Linear Scaling Relationships on Metal Catalysts via Ligand–Adsorbate Hydrogen Bonding. Journal of Physical Chemistry C, 2021, 125, 23791-23802.	1.5	4

#	Article	IF	CITATIONS
19	Relocation and reinforcement of the adhesive/composite interface with spontaneous amine-peroxide interfacial polymerization. Dental Materials, 2021, 37, 1865-1872.	1.6	0
20	Immobilization of "Capping Arene―Cobalt(II) Complexes on Ordered Mesoporous Carbon for Electrocatalytic Water Oxidation. ACS Catalysis, 2021, 11, 15068-15082.	5.5	8
21	Surface Hydrides on Fe <sub>2</sub> P Electrocatalyst Reduce CO <sub>2</sub> at Low Overpotential: Steering Selectivity to Ethylene Glycol. Journal of the American Chemical Society, 2021, 143, 21275-21285.	6.6	34
22	Atomic layer deposition of tungsten nitride films as protective barriers to hydrogen. Applied Surface Science, 2020, 507, 145019.	3.1	5
23	Stabilizing Hydrogen Adsorption through Theory-Guided Chalcogen Substitution in Chevrel-Phase Mo <sub>6</sub> X <sub>8</sub> (X=S, Se, Te) Electrocatalysts. ACS Applied Materials & Interfaces, 2020, 12, 35995-36003.	4.0	26
24	Computational and Experimental Evaluation of Peroxide Oxidants for Amine–Peroxide Redox Polymerization. Macromolecules, 2020, 53, 9736-9746.	2.2	5
25	A Synergistic Approach to Unraveling the Thermodynamic Stability of Binary and Ternary Chevrel Phase Sulfides. Chemistry of Materials, 2020, 32, 7044-7051.	3.2	10
26	Computationally Predicted High-Throughput Free-Energy Phase Diagrams for the Discovery of Solid-State Hydrogen Storage Reactions. ACS Applied Materials & Interfaces, 2020, 12, 48553-48564.	4.0	6
27	Modified Single Iteration Synchronous-Transit Approach to Bound Diffusion Barriers for Solid-State Reactions. Journal of Chemical Theory and Computation, 2020, 16, 5912-5922.	2.3	3
28	Predicting Spinel Disorder and Its Effect on Oxygen Transport Kinetics in Hercynite. ACS Applied Materials & Interfaces, 2020, 12, 23831-23843.	4.0	11
29	Highâ€Throughput Analysis of Materials for Chemical Looping Processes. Advanced Energy Materials, 2020, 10, 2000685.	10.2	18
30	Oxidation kinetics of hercynite spinels for solar thermochemical fuel production. Chemical Engineering Journal, 2020, 401, 126015.	6.6	17
31	High-Efficiency Radical Photopolymerization Enhanced by Autonomous Dark Cure. Macromolecules, 2020, 53, 5034-5046.	2.2	13
32	Solidâ€state sintering of coreâ€shell ceramic powders fabricated by particle atomic layer deposition. Journal of the American Ceramic Society, 2020, 103, 4101-4109.	1.9	1
33	Highly dispersed Co deposited on Al <sub>2</sub> O <sub>3</sub> particles via CoCp <sub>2</sub> + H <sub>2</sub> ALD. Nanotechnology, 2020, 31, 175703.	1.3	4
34	Inorganic Halide Double Perovskites with Optoelectronic Properties Modulated by Sublattice Mixing. Journal of the American Chemical Society, 2020, 142, 5135-5145.	6.6	62
35	Metalloradical intermediates in electrocatalytic reduction of CO <sub>2</sub> to CO: Mn <i>versus</i> Re bis-N-heterocyclic carbene pincers. Dalton Transactions, 2020, 49, 2053-2057.	1.6	18
36	Mn-Based Molecular Catalysts for the Electrocatalytic Disproportionation of CO <sub>2</sub> into CO and CO <sub>3</sub> <sup>2–</sup> . ACS Catalysis, 2020, 10, 1961-1968.	5.5	25

#	Article	IF	CITATIONS
37	Nonuniform Growth of Sub-2 Nanometer Atomic Layer Deposited Alumina Films on Lithium Nickel Manganese Cobalt Oxide Cathode Battery Materials. ACS Applied Nano Materials, 2019, 2, 6989-6997.	2.4	23
38	Enhancing Au/TiO <sub>2</sub> Catalyst Thermostability and Coking Resistance with Alkyl Phosphonic-Acid Self-Assembled Monolayers. ACS Applied Materials & Interfaces, 2019, 11, 41289-41296.	4.0	26
39	The role of decomposition reactions in assessing first-principles predictions of solid stability. Npj Computational Materials, 2019, 5, .	3.5	63
40	Independent Control of Singlet Oxygen and Radical Generation via Irradiation of a Two-Color Photosensitive Molecule. Macromolecules, 2019, 52, 4968-4978.	2.2	21
41	Continuous on-sun solar thermochemical hydrogen production via an isothermal redox cycle. Applied Energy, 2019, 249, 368-376.	5.1	49
42	Rational Design of Efficient Amine Reductant Initiators for Amine–Peroxide Redox Polymerization. Journal of the American Chemical Society, 2019, 141, 6279-6291.	6.6	19
43	High-Throughput Equilibrium Analysis of Active Materials for Solar Thermochemical Ammonia Synthesis. ACS Applied Materials & Interfaces, 2019, 11, 24850-24858.	4.0	21
44	The effect of ultrathin ALD films on the oxidation kinetics of SiC in high-temperature steam. Chemical Engineering Science, 2019, 201, 230-236.	1.9	5
45	Importance of proton-coupled electron transfer in cathodic regeneration of organic hydrides. Chemical Communications, 2019, 55, 5583-5586.	2.2	24
46	New tolerance factor to predict the stability of perovskite oxides and halides. Science Advances, 2019, 5, eaav0693.	4.7	778
47	Catalyst-free, aza-Michael polymerization of hydrazides: polymerizability, kinetics, and mechanistic origin of an α-effect. Polymer Chemistry, 2019, 10, 5790-5804.	1.9	9
48	Particle atomic layer deposition of alumina for sintering yttriaâ€stabilized cubic zirconia. Journal of the American Ceramic Society, 2019, 102, 2283-2293.	1.9	8
49	Benzimidazoles as Metal-Free and Recyclable Hydrides for CO <sub>2</sub> Reduction to Formate. Journal of the American Chemical Society, 2019, 141, 272-280.	6.6	67
50	Amine Induced Retardation of the Radical-Mediated Thiol–Ene Reaction via the Formation of Metastable Disulfide Radical Anions. Journal of Organic Chemistry, 2018, 83, 2912-2919.	1.7	32
51	Nanostructured mullite steam oxidation resistant coatings for silicon carbide deposited via atomic layer deposition. Journal of the American Ceramic Society, 2018, 101, 2493-2505.	1.9	11
52	Predicting Hydride Donor Strength via Quantum Chemical Calculations of Hydride Transfer Activation Free Energy. Journal of Physical Chemistry B, 2018, 122, 1278-1288.	1.2	15
53	Thermodynamic and kinetic hydricities of metal-free hydrides. Chemical Society Reviews, 2018, 47, 2809-2836.	18.7	103
54	Renewable Hydride Donors for the Catalytic Reduction of CO <sub>2</sub> : A Thermodynamic and Kinetic Study. Journal of Physical Chemistry B, 2018, 122, 10179-10189.	1.2	13

#	Article	IF	CITATIONS
55	Dynamic and Responsive DNA-like Polymers. Journal of the American Chemical Society, 2018, 140, 13594-13598.	6.6	45
56	Physical descriptor for the Gibbs energy of inorganic crystalline solids and temperature-dependent materials chemistry. Nature Communications, 2018, 9, 4168.	5.8	152
57	Bistable and photoswitchable states of matter. Nature Communications, 2018, 9, 2804.	5.8	111
58	A user's guide to the thiol-thioester exchange in organic media: scope, limitations, and applications in material science. Polymer Chemistry, 2018, 9, 4523-4534.	1.9	78
59	The Unified Electrochemical Band Diagram Framework: Understanding the Driving Forces of Materials Electrochemistry. Advanced Functional Materials, 2018, 28, 1803439.	7.8	8
60	Predicting kinetics of polymorphic transformations from structure mapping and coordination analysis. Physical Review Materials, 2018, 2, .	0.9	13
61	Implications of heterostructural alloying for enhanced piezoelectric performance of (Al,Sc)N. Physical Review Materials, 2018, 2, .	0.9	47
62	Adatom surface diffusion of catalytic metals on the anatase TiO <sub>2</sub> (101) surface. Physical Chemistry Chemical Physics, 2017, 19, 4541-4552.	1.3	28
63	Dihydropteridine/Pteridine as a 2H <sup>+</sup> /2e <sup>–</sup> Redox Mediator for the Reduction of CO <sub>2</sub> to Methanol: A Computational Study. Journal of Physical Chemistry B, 2017, 121, 4158-4167.	1.2	13
64	Solvent effects on the intramolecular charge transfer character of <i>N</i> , <i>N</i> â€diaryl dihydrophenazine catalysts for organocatalyzed atom transfer radical polymerization. Journal of Polymer Science Part A, 2017, 55, 3017-3027.	2.5	56
65	Intramolecular Charge Transfer and Ion Pairing in <i>N,N</i> -Diaryl Dihydrophenazine Photoredox Catalysts for Efficient Organocatalyzed Atom Transfer Radical Polymerization. Journal of the American Chemical Society, 2017, 139, 348-355.	6.6	207
66	Controlling the Surface Reactivity of Titania via Electronic Tuning of Self-Assembled Monolayers. ACS Catalysis, 2017, 7, 8351-8357.	5.5	30
67	A review and perspective of efficient hydrogen generation via solar thermal water splitting. Wiley Interdisciplinary Reviews: Energy and Environment, 2016, 5, 261-287.	1.9	168
68	Organocatalyzed atom transfer radical polymerization driven by visible light. Science, 2016, 352, 1082-1086.	6.0	649
69	Rapid Growth of Crystalline Mn <sub>5</sub> O <sub>8</sub> by Self-Limited Multilayer Deposition using Mn(EtCp) <sub>2</sub> and O <sub>3</sub> . ACS Applied Materials & Interfaces, 2016, 8, 18560-18569.	4.0	17
70	Organocatalyzed Atom Transfer Radical Polymerization Using <i>N</i> -Aryl Phenoxazines as Photoredox Catalysts. Journal of the American Chemical Society, 2016, 138, 11399-11407.	6.6	300
71	Degradation of Ethylene Carbonate Electrolytes of Lithium Ion Batteries via Ring Opening Activated by LiCoO <sub>2</sub> Cathode Surfaces and Electrolyte Species. ACS Applied Materials & Interfaces, 2016, 8, 26664-26674.	4.0	67
72	Band Diagram and Rate Analysis of Thin Film Spinel LiMn <sub>2</sub> O <sub>4</sub> Formed by Electrochemical Conversion of ALDâ€Grown MnO. Advanced Functional Materials, 2016, 26, 7895-7907.	7.8	37

#	Article	IF	CITATIONS
73	Aluminum Nitride Hydrolysis Enabled by Hydroxyl-Mediated Surface Proton Hopping. ACS Applied Materials & Interfaces, 2016, 8, 18550-18559.	4.0	21
74	First-Principles Analysis of Cation Diffusion in Mixed Metal Ferrite Spinels. Chemistry of Materials, 2016, 28, 214-226.	3.2	80
75	Growth and Characterization of Al <sub>2</sub> O <sub>3</sub> Atomic Layer Deposition Films on sp <sup>2</sup> -Graphitic Carbon Substrates Using NO <sub>2</sub> /Trimethylaluminum Pretreatment. ACS Applied Materials & Interfaces, 2015, 7, 12030-12037.	4.0	34
76	Sodium Charge Storage in Thin Films of MnO <sub>2</sub> Derived by Electrochemical Oxidation of MnO Atomic Layer Deposition Films. Journal of the Electrochemical Society, 2015, 162, A2753-A2761.	1.3	42
77	Charge Storage in Cation Incorporated α-MnO <sub>2</sub> . Chemistry of Materials, 2015, 27, 1172-1180.	3.2	122
78	Solvent Control of Surface Plasmon-Mediated Chemical Deposition of Au Nanoparticles from Alkylgold Phosphine Complexes. ACS Applied Materials & Interfaces, 2015, 7, 13384-13394.	4.0	8
79	Intrinsic Material Properties Dictating Oxygen Vacancy Formation Energetics in Metal Oxides. Journal of Physical Chemistry Letters, 2015, 6, 1948-1953.	2.1	103
80	Predicting the solar thermochemical water splitting ability and reaction mechanism of metal oxides: a case study of the hercynite family of water splitting cycles. Energy and Environmental Science, 2015, 8, 3687-3699.	15.6	68
81	Mechanisms of LiCoO <sub>2</sub> Cathode Degradation by Reaction with HF and Protection by Thin Oxide Coatings. ACS Applied Materials & amp; Interfaces, 2015, 7, 24265-24278.	4.0	98
82	Mechanism of hydrofluoric acid formation in ethylene carbonate electrolytes with fluorine salt additives. Journal of Power Sources, 2015, 297, 427-435.	4.0	35
83	Catalytic Reduction of CO <sub>2</sub> by Renewable Organohydrides. Journal of Physical Chemistry Letters, 2015, 6, 5078-5092.	2.1	59
84	Extracting Kinetic Information from Complex Gas–Solid Reaction Data. Industrial & Engineering Chemistry Research, 2015, 54, 4113-4122.	1.8	26
85	Electronic and dielectric properties of Ruddlesden–Popper type and Magnéli type SrTiO3. Computational Materials Science, 2015, 96, 223-228.	1.4	15
86	Tunable Oxygen Vacancy Formation Energetics in the Complex Perovskite Oxide Sr <sub><i>x</i></sub> La <sub>1–<i>x</i></sub> Mn <sub><i>y</i></sub> Al <sub>1–<i>y</i></sub> O <sub>3 Chemistry of Materials, 2014, 26, 6595-6602.</sub>	}< <b>ås⊵</b> b>.	90
87	Reduction of CO <sub>2</sub> to Methanol Catalyzed by a Biomimetic Organo-Hydride Produced from Pyridine. Journal of the American Chemical Society, 2014, 136, 16081-16095.	6.6	131
88	Increasing the Photocatalytic Activity of Anatase TiO <sub>2</sub> through B, C, and N Doping. Journal of Physical Chemistry C, 2014, 118, 27415-27427.	1.5	55
89	Visible-Light Organic Photocatalysis for Latent Radical-Initiated Polymerization via 2e <sup>–</sup> /1H <sup>+</sup> Transfers: Initiation with Parallels to Photosynthesis. Journal of the American Chemical Society, 2014, 136, 7418-7427.	6.6	78
90	Oxide enthalpy of formation and band gap energy as accurate descriptors of oxygen vacancy formation energetics. Energy and Environmental Science, 2014, 7, 1996.	15.6	109

#	Article	IF	CITATIONS
91	Bulk and Surface Tunneling Hydrogen Defects in Alumina. Physical Review Letters, 2013, 111, 065901.	2.9	51
92	Roles of the Lewis Acid and Base in the Chemical Reduction of CO <sub>2</sub> Catalyzed by Frustrated Lewis Pairs. Inorganic Chemistry, 2013, 52, 10062-10066.	1.9	58
93	Efficient Generation of H <sub>2</sub> by Splitting Water with an Isothermal Redox Cycle. Science, 2013, 341, 540-542.	6.0	296
94	Mechanistic Basis for High Stereoselectivity and Broad Substrate Scope in the (salen)Co(III)-Catalyzed Hydrolytic Kinetic Resolution. Journal of the American Chemical Society, 2013, 135, 15595-15608.	6.6	115
95	A Correlated Electron View of Singlet Fission. Accounts of Chemical Research, 2013, 46, 1339-1347.	7.6	150
96	The Effect of N and B Doping on Graphene and the Adsorption and Migration Behavior of Pt Atoms. Journal of Physical Chemistry C, 2013, 117, 10523-10535.	1.5	71
97	Mechanism of Homogeneous Reduction of CO <sub>2</sub> by Pyridine: Proton Relay in Aqueous Solvent and Aromatic Stabilization. Journal of the American Chemical Society, 2013, 135, 142-154.	6.6	151
98	Growth of Pt Particles on the Anatase TiO <sub>2</sub> (101) Surface. Journal of Physical Chemistry C, 2012, 116, 12114-12123.	1.5	63
99	Effect of Surface Deposited Pt on the Photoactivity of TiO <sub>2</sub> . Journal of Physical Chemistry C, 2012, 116, 10138-10149.	1.5	92
100	Molecular Layer Deposition of Conductive Hybrid Organic-Inorganic Thin Films Using Diethylzinc and Hydroquinone. ECS Transactions, 2011, 33, 191-195.	0.3	33
101	Atomic Layer Deposition of Tantalum Nitride Using A Novel Precursor. Journal of Physical Chemistry C, 2011, 115, 11507-11513.	1.5	25
102	Reactions of Amino Acids on the Si(100)-2×1 Surface. Journal of Physical Chemistry C, 2011, 115, 7477-7486.	1.5	13
103	Effects of Water and Formic Acid Adsorption on the Electronic Structure of Anatase TiO <sub>2</sub> (101). Journal of Physical Chemistry C, 2011, 115, 2738-2749.	1.5	41
104	Dynamic Mechanisms for Ammonia Borane Thermolysis in Solvent: Deviation from Gas-Phase Minimum-Energy Pathways. Journal of Physical Chemistry Letters, 2011, 2, 276-281.	2.1	27
105	Effect of interface structure on the Ru on HfO2 work function. Journal of Materials Science, 2010, 45, 4924-4928.	1.7	2
106	Singlet fission in pentacene through multi-exciton quantum states. Nature Chemistry, 2010, 2, 648-652.	6.6	356
107	Reaction Mechanism, Bonding, and Thermal Stability of 1-Alkanethiols Self-Assembled on Halogenated Ge Surfaces. Langmuir, 2010, 26, 8419-8429.	1.6	22
108	Simultaneous Two-Hydrogen Transfer as a Mechanism for Efficient CO <sub>2</sub> Reduction. Inorganic Chemistry, 2010, 49, 8724-8728.	1.9	70

#	Article	IF	CITATIONS
109	Excited states of methylene from quantum Monte Carlo. Journal of Chemical Physics, 2009, 131, 124103.	1.2	70
110	The Role of Free Nâ€Heterocyclic Carbene (NHC) in the Catalytic Dehydrogenation of Ammonia–Borane in the Nickel NHC System. Angewandte Chemie - International Edition, 2009, 48, 2201-2205.	7.2	115
111	Oligomerization and Autocatalysis of NH2BH2 with Ammoniaâ^'Borane. Inorganic Chemistry, 2009, 48, 1069-1081.	1.9	108
112	Catalytic Dehydrogenation of Ammonia Borane at Ni Monocarbene and Dicarbene Catalysts. Inorganic Chemistry, 2009, 48, 5418-5433.	1.9	72
113	Formation of Alkanethiolate Self-Assembled Monolayers at Halide-Terminated Ge Surfaces. Langmuir, 2009, 25, 2013-2025.	1.6	38
114	Adsorption of Organic Matter at Mineral/Water Interfaces: 7. ATR-FTIR and Quantum Chemical Study of Lactate Interactions with Hematite Nanoparticles. Langmuir, 2008, 24, 6683-6692.	1.6	55
115	Quantum dot properties in the multiband envelope-function approximation using boundary conditions based upon first-principles quantum calculations. Physical Review B, 2008, 77, .	1.1	5
116	Atomic Layer Deposition of Hafnium Oxide from Hafnium Chloride and Water. Journal of the American Chemical Society, 2008, 130, 11996-12006.	6.6	45
117	Comparison of DFT Methods for Molecular Orbital Eigenvalue Calculations. Journal of Physical Chemistry A, 2007, 111, 1554-1561.	1.1	693
118	A Detailed Theoretical Study of the Mechanism and Energetics of Methane to Methanol Conversion by Cisplatin and Catalytica. Organometallics, 2007, 26, 793-809.	1.1	49
119	The role of ammonia in atomic layer deposition of tungsten nitride. Applied Physics Letters, 2007, 90, 173120.	1.5	17
120	Attachment of Alanine and Arginine to the Ge(100)-2×1 Surface. Journal of Physical Chemistry C, 2007, 111, 3692-3699.	1.5	18
121	Carbonâ^'Oxygen Coupling in the Reaction of Formaldehyde on Ge(100)-2×1. Journal of Physical Chemistry C, 2007, 111, 1739-1746.	1.5	12
122	First-Principles Investigation of the Structure, Energetics, and Electronic Properties of Ru/HfO2Interfaces. Journal of Physical Chemistry C, 2007, 111, 9203-9210.	1.5	11
123	Carbon Dioxide Reduction by Pincer Rhodium η2-Dihydrogen Complexes: Hydrogen-Binding Modes and Mechanistic Studies by Density Functional Theory Calculations. Organometallics, 2007, 26, 508-513.	1.1	62
124	Catalyzed Dehydrogenation of Ammonia–Borane by Iridium Dihydrogen Pincer Complex Differs from Ethane Dehydrogenation. Angewandte Chemie - International Edition, 2007, 46, 8153-8156.	7.2	194
125	First-Principles Investigation of Hydroxylated Monoclinic HfO2 Surfaces. Chemistry of Materials, 2006, 18, 3397-3403.	3.2	30
126	First-principles calculations of structural and electronic properties of monoclinic hafnia surfaces. Physical Review B, 2006, 73, .	1.1	71

#	Article	IF	CITATIONS
127	Density Functional Theory Calculations of Tiâ^'TEMPO Complexes:Â Influence of Ancillary Ligation on the Strength of the Tiâ^'O Bond. Organometallics, 2006, 25, 3317-3323.	1.1	20
128	Non-growth ligand exchange reactions in atomic layer deposition of HfO2. Chemical Physics Letters, 2006, 421, 215-220.	1.2	23
129	A chemical mechanism for nitrogen incorporation into HfO2 ALD films using ammonia and alkylamide as precursors. Surface Science, 2005, 591, L280-L285.	0.8	11
130	Atomic layer deposition of hafnium nitrides using ammonia and alkylamide precursors. Chemical Physics Letters, 2005, 407, 272-275.	1.2	11
131	First-principles calculation of free Si(100) surface impurity enrichment. Applied Physics Letters, 2005, 87, 232101.	1.5	7
132	Atomic layer deposition of high-lº dielectrics on nitrided silicon surfaces. Applied Physics Letters, 2005, 86, 192110.	1.5	15
133	First-principles calculation of intrinsic defect formation volumes in silicon. Physical Review B, 2005, 72, .	1.1	76
134	Homolysis of Weak Tiâ~'O Bonds:Â Experimental and Theoretical Studies of Titanium Oxygen Bonds Derived from Stable Nitroxyl Radicals. Journal of the American Chemical Society, 2005, 127, 3807-3816.	6.6	49
135	Initial Nitridation of the Ge(100)-2 × 1 Surface by Ammonia. Langmuir, 2005, 21, 5230-5232.	1.6	18
136	Density Functional Theory Study of the Geometry, Energetics, and Reconstruction Process of Si(111) Surfaces. Langmuir, 2005, 21, 12404-12414.	1.6	21
137	In-Situ Infrared Spectroscopy and Density Functional Theory Modeling of Hafnium Alkylamine Adsorption on Siâ^'OH and Siâ^'H Surfaces. Chemistry of Materials, 2005, 17, 5305-5314.	3.2	55
138	Predicting ionic conductivity of solid oxide fuel cell electrolyte from first principles. Journal of Applied Physics, 2005, 98, 103513.	1.1	162
139	Indirect adsorbate–adsorbate interactions mediated through the surface electronic structure of the Si(100) surface. Journal of Chemical Physics, 2004, 120, 1555-1559.	1.2	33
140	A quantum chemical study of ZrO2 atomic layer deposition growth reactions on the SiO2 surface. Surface Science, 2004, 550, 199-212.	0.8	45
141	Surface reaction mechanisms for atomic layer deposition of silicon nitride. Surface Science, 2004, 557, 159-170.	0.8	34
142	Atomic Layer Deposition of HfO2 Using Alkoxides as Precursors. Journal of Physical Chemistry B, 2004, 108, 15150-15164.	1.2	28
143	A Density Functional Theory Study on the Effect of Ge Alloying on Hydrogen Desorption from SiGe Alloy Surfaces. Journal of Physical Chemistry B, 2004, 108, 6336-6350.	1.2	9
144	Calculating Cumulene/Poly-yne Isomerization Energies. Journal of Physical Chemistry A, 2004, 108, 4030-4035.	1.1	12

#	Article	IF	CITATIONS
145	A DFT Study of the Al2O3Atomic Layer Deposition on SAMs:Â Effect of SAM Termination. Chemistry of Materials, 2004, 16, 646-653.	3.2	83
146	Quantum Chemistry Based Statistical Mechanical Model of Hydrogen Desorption from Si(100)-2 × 1, Ge(100)-2 × 1, and SiGe Alloy Surfaces. Journal of Physical Chemistry B, 2004, 108, 18243-18253.	1.2	9
147	Initial Oxidation and Hydroxylation of the Ge(100)-2×1 Surface by Water and Hydrogen Peroxide. Langmuir, 2004, 20, 7604-7609.	1.6	16
148	A Quantum Chemical Study of the Atomic Layer Deposition of Al2O3 Using AlCl3 and H2O as Precursors. Journal of Physical Chemistry B, 2004, 108, 5718-5725.	1.2	64
149	Adsorption of organic matter at mineral/water interfaces: I. ATR-FTIR spectroscopic and quantum chemical study of oxalate adsorbed at boehmite/water and corundum/water interfaces. Geochimica Et Cosmochimica Acta, 2004, 68, 4505-4518.	1.6	120
150	A shock tube study of the reaction NH2 + CH4 ? NH3 + CH3 and comparison with transition state theory. International Journal of Chemical Kinetics, 2003, 35, 304-309.	1.0	23
151	Temperature and pressure dependence of the reaction of OH and CO: Master equation modeling on a high-level potential energy surface. International Journal of Chemical Kinetics, 2003, 35, 464-474.	1.0	49
152	Kinetic lattice Monte Carlo simulations of processes on the silicon (100) surface. Physica E: Low-Dimensional Systems and Nanostructures, 2003, 19, 183-187.	1.3	3
153	Reactions of Nitriles at Semiconductor Surfaces. Journal of Physical Chemistry B, 2003, 107, 12256-12267.	1.2	35
154	Quantum Chemical Study of Zirconium Oxide Deposition on the Si(100)â^'(2×1) Surface. Journal of Physical Chemistry B, 2003, 107, 9319-9324.	1.2	31
155	Competition and Selectivity in the Reaction of Nitriles on Ge(100)â^2×1. Journal of the American Chemical Society, 2003, 125, 4928-4936.	6.6	40
156	Reactions of Cyclic Aliphatic and Aromatic Amines on Ge(100)-2×1 and Si(100)-2×1. Journal of Physical Chemistry B, 2003, 107, 4982-4996.	1.2	84
157	The mechanism of HF/H[sub 2]O chemical etching of SiO[sub 2]. Journal of Chemical Physics, 2002, 116, 275.	1.2	99
158	Quantum chemical study of the elementary reactions in zirconium oxide atomic layer deposition. Applied Physics Letters, 2002, 81, 304-306.	1.5	54
159	Atomic layer deposition of hafnium oxide: A detailed reaction mechanism from first principles. Journal of Chemical Physics, 2002, 117, 1931-1934.	1.2	99
160	Quantum chemical study of the mechanism of aluminum oxide atomic layer deposition. Applied Physics Letters, 2002, 80, 3304-3306.	1.5	178
161	Mechanism of atomic layer deposition of SiO2 on the silicon (100)-2×1 surface using SiCl4 and H2O as precursors. Journal of Applied Physics, 2002, 91, 3408-3414.	1.1	55
162	A quantum chemical study of the self-directed growth mechanism of styrene and propylene molecular nanowires on the silicon (100) 2×1 surface. Journal of Chemical Physics, 2002, 116, 9907-9913.	1.2	56

#	Article	IF	CITATIONS
163	Modeling Copper Diffusion in Silicon Oxide, Nitride, and Carbide. Materials Research Society Symposia Proceedings, 2002, 716, 841.	0.1	5
164	Proton Transfer Reactions on Semiconductor Surfaces. Journal of the American Chemical Society, 2002, 124, 4027-4038.	6.6	152
165	Competition and Selectivity of Organic Reactions on Semiconductor Surfaces:Â Reaction of Unsaturated Ketones on Si(100)-2×1 and Ge(100)-2×1. Journal of the American Chemical Society, 2002, 124, 8990-9004.	6.6	87
166	Density Functional Theory Study of Atomic Nitrogen on the Si(100)â^'(2 × 1) Surface. Journal of Physical Chemistry B, 2002, 106, 2643-2648.	1.2	15
167	Atomistic mechanism of the initial oxidation of the clean Si(100)-(2×1) surface by O2 and SiO2 decomposition. Journal of Chemical Physics, 2002, 116, 5774-5780.	1.2	39
168	Topological Disorder and Reactivity of Borosilicate Glasses:Â Quantum Chemical Calculations and170 and11B NMR Study. Journal of Physical Chemistry B, 2001, 105, 12583-12595.	1.2	64
169	Prediction of transition state barriers and enthalpies of reaction by a new hybrid density-functional approximation. Journal of Chemical Physics, 2001, 115, 11040-11051.	1.2	177
170	Reactions of methylamines at the Si(100)-2×1 surface. Journal of Chemical Physics, 2001, 114, 10170-10180.	1.2	130
171	DFT Study of the Adsorption of Chlorosilanes on the Si(100)-2 × 1 Surface. Journal of Physical Chemistry B, 2001, 105, 12068-12075.	1.2	25
172	Use of quantum methods for a consistent approach to combustion modelling: Hydrocarbon bond dissociation energies. Faraday Discussions, 2001, 119, 173-189.	1.6	45
173	Effect of a Methyl-Protecting Group on the Adsorption of Pyrrolidine on Si(100)-2 × 1. Journal of Physical Chemistry B, 2001, 105, 3295-3299.	1.2	33
174	Example of a Thermodynamically Controlled Reaction on a Semiconductor Surface:Â Acetone on Ge(100)-2 × 1. Journal of Physical Chemistry B, 2001, 105, 12559-12565.	1.2	69
175	Use of Quantum Methods with Transition State Theory: Application to H-Atom Metathesis Reactionsâ€. Journal of Physical Chemistry A, 2001, 105, 1669-1675.	1.1	30
176	The effect of an electric field on the chemical vapour deposition of (100) diamond. Nanotechnology, 2001, 12, 258-264.	1.3	1
177	Ab initiostudy of the initial growth mechanism of silicon nitride onSi(100)â^'(2×1)usingNH3. Physical Review B, 2001, 64, .	1.1	49
178	Theoretical study of the chemical vapor deposition of (100) silicon from silane. Physical Review B, 2001, 64, .	1.1	30
179	A Theoretical Study of the Structure and Thermochemistry of 1,3-Butadiene on the Ge/Si(100)-2 × 1 Surface. Journal of Physical Chemistry A, 2000, 104, 2457-2462.	1.1	74
180	A theoretical study of the chemical vapor deposition of (100) diamond: An explanation for the slow growth of the (100) surface. Journal of Chemical Physics, 2000, 113, 7582-7587.	1.2	21

#	Article	IF	CITATIONS
181	A density functional theory study of the nonlocal effects of NH3 adsorption and dissociation on Si(100)-(2×1). Surface Science, 2000, 469, 9-20.	0.8	110
182	Ab Initio Study of Adsorption and Decomposition of NH3on Si(100)-(2×1). Journal of Physical Chemistry B, 2000, 104, 2527-2533.	1.2	118
183	Theoretical study of the Cl-passivated Si(111) surface. Surface Science, 1999, 430, 116-125.	0.8	13
184	Cycloaddition of Cyclopentadiene and Dicyclopentadiene on Si(100)-2×1: Comparison of Monomer and Dimer Adsorption. Journal of Physical Chemistry B, 1999, 103, 6803-6808.	1.2	50
185	The surface-radical-surface-olefin recombination step for CVD growth of diamond. Calculation of the rate constant from first principles. Chemical Physics Letters, 1995, 247, 359-365.	1.2	10
186	Hessian biased force field for polysilane polymers. The Journal of Physical Chemistry, 1995, 99, 13321-13333.	2.9	13
187	Hydrolysis protection and sintering of aluminum nitride powders with yttria nanofilms. Journal of the American Ceramic Society, 0, , .	1.9	4
188	X-ray absorption spectroscopy insights on the structure anisotropy and charge transfer in Chevrel Phase chalcogenides. Physical Chemistry Chemical Physics, 0, , .	1.3	0